See related Commentary on page 2205

Tumorigenesis and Neoplastic Progression

Differential Regulation and Predictive Potential of MacroH2A1 Isoforms in Colon Cancer

Judith C. Sporn and Barbara Jung

From the Department of Medicine and Robert H. Lurie Comprehensive Cancer Center, Northwestern University Feinberg School of Medicine, Chicago, Illinois

Histone variant macroH2A1 has two splice isoforms, macroH2A1.1 and macroH2A1.2, with tissue- and cell-specific expression patterns. Although macroH2A1.1 is mainly found in differentiated, nonproliferative tissues, macroH2A1.2 is more generally expressed, including in tissues with ongoing cell proliferation. Consistently, studies in breast and lung cancer have demonstrated a strong correlation between macroH2A1.1 levels and proliferation, which is not the case for macroH2A1.2. This is the first study to assess the differential regulation and predictive potential of macroH2A1 isoforms in colon cancer. We found that macroH2A1.1 mRNA was down-regulated in primary colorectal cancer samples compared to matched normal colon tissue, whereas macroH2A1.2 was up-regulated. At the protein level, down-regulation of macroH2A1.1 correlated significantly with patient outcome ($P = 0.0012$), and loss of macroH2A1.1 was associated with a worse outcome. Over the course of Caco-2 cell differentiation, macroH2A1.1 was up-regulated at both the RNA and protein levels, whereas macroH2A1.2 was slightly down-regulated at the RNA level and stable at the protein level. These changes were accompanied by an antiproliferative phenotype exhibiting features of cellular senescence. Loss of macroH2A1.1 *in vitro* was characterized by a phenotype associated with cell growth and metastasis. These data demonstrate that macroH2A1 isoforms are differentially regulated in colon cancer, reflecting the degree of cellular differentiation. Notably, macroH2A1.1 expression predicts survival in colon cancer, thus identifying macroH2A1.1 as a novel colon cancer biomarker. *(Am J Pathol 2012, 180: 2516–2526; http://dx.doi.org/10.1016/j.ajpath.2012.02.027)*

Histone variants are nonallelic isoforms that replace conventional histones within certain chromatin domains. By altering the structure of the nucleosome, they contribute select functions to chromatin. MacroH2A1 is a rather special histone variant consisting of two domains, the N-terminal histone fold and a C-terminal non-histone fold, the *macro* domain.[1] The *macro* domain, a 25-kDa-sized globular module, distinguishes macroH2A from all known core histones. Although the *macro* domain itself is conserved among archaebacteria and viruses,[2,3] histone variant macroH2A appears to be restricted to vertebrates, among which it is highly conserved.[4] There are two isoforms, macroH2A1.1 and macroH2A1.2, produced by alternative splicing of the *H2AFY* gene, which differ in one single exon. Both isoforms have been associated with states of silencing and transcriptional repression, such as facultative heterochromatin,[5] centromeric regions,[6] and X inactivation,[7] suggesting overlapping functions for both splice variants. Yet, various studies reveal isoform-specific properties. *In vitro*, the *macro* domain of macroH2A1.1, but not macroH2A1.2, binds ADP-ribose and related NAD metabolites.[3] Studies in mice and rats show a differential expression pattern of macroH2A1 isoforms in various tissues as well as during development. Overall, macroH2A1.1 is mainly expressed in differentiated, nonproliferative tissues, whereas the second splice variant, macroH2A1.2, is more generally expressed, including in tissues with ongoing cell proliferation.[8,9]

These findings are supported by studies in breast and lung cancer, revealing a strong correlation between macroH2A1.1 levels and proliferation, which has not been found for macroH2A1.2. High levels of macroH2A1.1 are associated with slowly proliferating lung cancers, whereas highly proliferating tumors have markedly decreased

macroH2A1.1 levels. Conversely, macroH2A1.2 levels have been found to be similar in all tumors independently of proliferation.[10] Notably, expression of macroH2A1.1 has been shown to be predictive of lung cancer recurrence, identifying histone variant macroH2A1.1 as a novel biomarker in lung cancer.[10]

We now show that expression of macroH2A1.1 can predict outcome in colon cancer, suggesting that macroH2A1.1 could also serve as a useful prognostic biomarker in colon cancer. We observed an increase of macroH2A1.1 mRNA and protein over the course of differentiation that is accompanied by an antiproliferative phenotype exhibiting features of cellular senescence. Loss of macroH2A1 *in vitro* is characterized by a phenotype favoring proliferation and metastasis.

Materials and Methods

Reverse Transcription and Quantitative Real-Time PCR

RNA from 15 human colorectal cancer samples and 15 matched normal colon samples was acquired from Biochain (Hayward, CA). RNA quality was assessed with the Agilent Bio-Chip (Agilent, Santa Clara, CA) (RNA integrity number >6.5). One microgram of RNA of each sample was reverse-transcribed using the Superscript III First-Strand Synthesis SuperMix and Oligo(dT)$_{20}$ primers by Invitrogen (Carlsbad, CA) according to the manufacturer's instruction. Reverse transcription was followed by RNase H digest (New England Biolabs, Ipswich, MA). cDNA served as the quantitative PCR (qPCR) template. To quantify the expression of the two macroH2A1 splice variants, we performed SYBR Green quantitative real-time PCR assays. Primer 3[11] and Primer Express software V3.0 (Applied Biosystems, Foster City, CA) were used to design exon-spanning qPCR primer pairs specific for macroH2A1.1 (5′-GCCTCTTCCTTGGCCA GAA-3′ and 5′-CACTGTCGATCGAGGCAATG-3′) and macroH2A1.2 (5′-CTTTGAGGTGGAGGCCATAA-3′ and 5′-TCTTCTCCAGCGTGTTTCCT-3′). qPCR reactions were performed in triplicate using the Fast SYBR Green Master Mix (Applied Biosystems) with a total reaction volume of 20 μL and primer concentrations of 100 nmol/L. The experiments were run on a 7900HT Fast Real-Time PCR System (Applied Biosystems) following the standard protocol for the Fast SYBR Green Master Mix. A dissociation stage was added to the run protocol. PCR efficiency was established by calibration curves using cDNA from Caco-2 cells as a template. Control reactions were performed using genomic DNA as a template and no template; both resulted in no amplification. Dissociation curves were analyzed to ensure the specificity of the detected signal. A common threshold was determined for both splice variant runs. Quantification cycle values for each sample were transformed to relative quantities, corrected for efficiency.

For normalization purposes, we quantified the expression of five reference genes: *L19*, *GAPDH*, *B2M*, *RPLPO*, *HPRT1*. *L19* was quantified in a SYBR Green assay ac-cording to the method described above, using the following primers at a concentration of 100 nmol/L: (5′-AC-CCCAATGAGACCAATGAAAT-3′ and 5′-CAGCCCATC TTTGATGAGCTT-3′). The other four reference genes were quantified using Pre-Developed TaqMan Assay Reagents (4333764F, 4333766F, 4333761F, 4333768F; Applied Biosystems) and the TaqMan Gene Expression Master Mix (Applied Biosystems). The experiments were run on the same instrument following the standard protocol and conditions as outlined for the TaqMan Gene Expression Master Mix. Quantification cycle values for each sample were transformed to relative quantities, corrected for efficiency, and the geometric mean of the five reference genes was calculated for each sample. The relative quantity of each sample determined in the splice variant runs was normalized to the geometric mean of the reference genes.[12] The ratio of the normalized relative quantity of each cancer sample and its matched normal colon sample was calculated and plotted on a graph with a logarithmic scale, depicting the fold expression change in cancer versus normal tissue. In a second graph, we plotted the normalized relative quantities for each matched pair sample in a dot-and-line diagram and performed a paired samples *t*-test using the MedCalc software (version 11.4.4.0).

As a further quality control, we conducted a 3′:5′ assay to ensure the integrity of the RNA/cDNA and used the Solaris qPCR control kit (Thermo Scientific, Rockford, IL) to exclude any relevant inhibition of the reactions.

Immunohistochemistry

A paraffin-embedded tissue multiarray containing 59 primary colorectal cancer samples was acquired from Imgenex (San Diego, CA) and assessed for protein expression of macroH2A1.1 and macroH2A1.2. Slides were probed with isoform-specific rabbit polyclonal antibodies against macroH2A1.1 (#4160; Cell Signaling Technology, Danvers, MA) and macroH2A1.2 (YenZym Antibodies, South San Francisco, CA). The antibody against macroH2A1.2 was custom made and raised against a peptide representing the alternatively spliced exon specific for macroH2A1.2. Immunohistochemistry was performed according to the standard protocol for the Vectastain Universal Elite ABC kit (Vector Laboratories, Burlingame, CA), detected with diaminobenzidine (Vector Laboratories), and counterstained with Mayer's hematoxylin (Sigma-Aldrich, St. Louis, MO). Slides were scanned using the Aperio Scanscope XT instrument at ×20 (Aperio, Vista, CA). Tumor cells within each core were selected for analysis using the pen tool within the WebScope viewing software. The Aperio Nuclear tool (Nuclear Analysis v9.1 algorithm, see Supplemental Table S1 at *http://ajp.amjpathol.org*) was used to analyze the nuclear staining intensity of the cancer cells within each core. Fifty patient samples with good-quality tissue in the cores were included in the analysis (for patient characteristics, see Supplemental Table S2 at *http://ajp.amjpathol.org*). Three intensity levels were discerned by the program: 3 (strong

nuclear staining); 2 (intermediate nuclear staining); and 1 (weak or no staining). In addition, adjacent normal tissue found in the cores was analyzed accordingly for the expression of macroH2A1.1 and macroH2A1.2.

To assess macroH2A1.1 expression levels in fetal and adult tissue, we performed immunohistochemistry against macroH2A1.1 on a slide containing adult human heart tissue as well as heart tissue from a fetus at 16 weeks (Biochain). We did not perform staining against macroH2A1.2, as striated muscle lacks expression of macroH2A1.2.

Cell Culture Differentiation Experiment

Caco-2 cells, derived from human colorectal carcinoma, were obtained from ATCC (Manassas, VA). Caco-2 cells were tested for mycoplasma infection using the PCR Mycoplasma Detection Set (Takara, Otsu, Japan) and authenticated by short tandem repeat profiling using the PowerPlex 1.2 System (Promega, Fitchburg, WI). Caco-2 cells were grown in Iscove's Modification of Dulbecco's modified Eagle's medium (Mediatech, Manassas, VA) supplemented with 1% (v/v) penicillin/streptomycin and 10% (v/v) heat-inactivated fetal calf serum. For differentiation experiments, cells were plated at passage 16 into 100-mm cell culture dishes (Corning, Corning, New York), at a density of ~5000 cells/cm². Caco-2 cultures were allowed to undergo proliferation and differentiation, and were harvested on days: 1, 3, 5, 7, 14, 21, and 28. For each day, triplicate cell cultures were harvested. Cells were washed with ice-cold PBS, collected by scraping, divided into two tubes, and then centrifuged. One cell pellet was flash-frozen in liquid nitrogen and stored at −80°C until further use; the second pellet was used for immediate total RNA extraction using the RNeasy Plus Mini Kit (Qiagen, Valencia, CA), including an on-column DNAseI digest as outlined by the manual. RNA quality of the samples was determined by Agilent Bio-Chip (RNA integrity number >9.5). Reverse transcription and quantification by qPCR were performed as described above.

Histone Extraction and Western Blot Analysis

After completion of the differentiation experiment, flash-frozen samples were used for acid extraction of histones using the EpiQuik Total Histone Extraction Kit (Epigentek, Farmingdale, NY). Protein concentration was determined by Quick Start Bradford Protein Assay with BSA as a standard (BioRad, Hercules, CA). Three micrograms of total histone per sample were loaded on a 4% to 20% SDS gel (Expedeon, San Diego, CA), run under reducing conditions and blotted on a polyvinylidene difluoride membrane (Millipore, Billerica, MA). Blots were incubated with the above-mentioned antibodies against macroH2A1.1 and macroH2A1.2, followed by secondary incubation with horseradish peroxidase–linked anti-rabbit antibody (#7074; Cell Signaling) using the SNAP i.d. Protein Detection System (Millipore). Histone H3 was used as a loading control (sc-10809; Santa Cruz Biotechnol-

ogy, Santa Cruz, CA). Signal was detected with Super-Signal West Pico Chemiluminescent Substrate (Thermo Fisher Scientific) and visualized with the LAS-3000 (Fujifilm USA, Valhalla, NY).

PCR Arrays

RT² Profiler PCR Arrays were acquired from SABiosciences (Frederick, MD) to analyze the expression of genes associated with cell cycle regulation (PAHS-020) and cellular senescence (PAHS-050). To compare the expression of these genes in proliferating cells (low macroH2A1.1 levels) with differentiated cells (high macroH2A1.1 expression), we used Caco-2 RNA from day 1 (low macroH2A1.1 expression) and day 21 (high macroH2A1.1 expression) of the differentiation experiment. RNA was reverse transcribed, and PCR arrays were used in combination with the special formulated and instrument-specific SYBR Green real-time PCR master mixes (SABiosciences) according to the manufacturer's instructions. Data were analyzed using the online PCR Array Data Analysis tool by SABiosciences. Three biological replicates were used to determine the mean expression in each group, and the geometric mean over five housekeeping genes on each array was used for normalization. The fold change of normalized expression between proliferating and differentiated Caco-2 cells was calculated by the analysis tool, and a *P* value was determined. All genes that showed an expression change greater than ±1.5-fold along with *P* values smaller than 0.05 were depicted on a graph with a logarithmic scale.

All control features implemented on the array were passed. No genomic DNA contamination was detected. Reverse transcription controls indicated no inhibition of the reaction. Positive PCR controls demonstrated inter-well and intraplate consistency. Dissociation curves showed specificity of the detected signal.

siRNA Knockdown of MacroH2A1.1 and MacroH2A1.2

FET cells (a generous gift from Michael Brattain, University of Nebraska, Omaha, NE) were cultured in F12/Dulbecco's modified Eagle's medium (Mediatech) supplemented with 10% (v/v) heat-inactivated fetal calf serum. Cells were tested for mycoplasma infection and authenticated as mentioned above. Specific small-interfering RNAs (siRNAs) for macroH2A1.1 and macroH2A1.2 and a non-targeting control siRNA (Ambion, Austin, TX) were transiently delivered at a final concentration of 25 nmol/L via electroporation using the AMAXA Nucleofector (Lonza, Basel, Switzerland) in six-well plates at a density of 2×10^6 cells per well. Transfection efficiency was confirmed using the pmaxGFP Control Vector (Lonza). Seventy-two hours post transfection, FET cells were lysed for subsequent RNA and histone extraction as described above. Knockdown was confirmed by quantitative real-time PCR and Western blot analysis according to the methods above. RNA from three biolog-
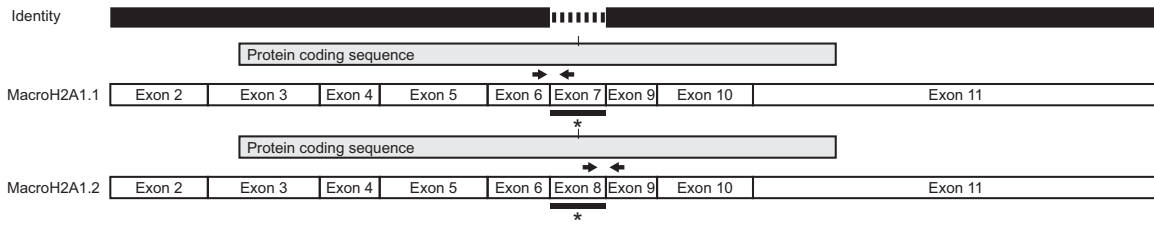
Figure 1. Schematic of human macroH2A1 isoforms: Alternatively spliced exons are marked with an **asterisk**. Locations of PCR primers are marked by **arrows**. Exons are numbered according to the National Center for Biotechnology Information Reference Sequence database.

ical replicates of each knockdown and control experiment was used for real-time PCR gene expression analysis using the PCR arrays by SABiosciences, as described in detail earlier. All genes that showed an expression change greater than ±1.5-fold along with a P value smaller than 0.05 (comparing knockdown versus control FET cells) were depicted on a graph with a logarithmic scale.

Statistical Analysis

Survival data for the tissue multiarrays was provided by Imgenex. The relationship between macroH2A1.1 and macroH2A1.2 expression and overall survival was as-

sessed by a log-rank test in a univariate analysis using the MedCalc software (version 11.4.4.0).

Results

MacroH2A1.1 Expression Is Down-Regulated in Colon Cancer Compared to Matched Normal Colon Tissue
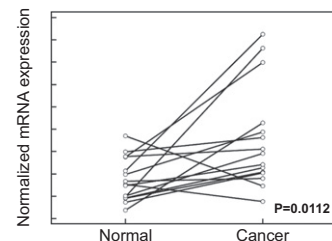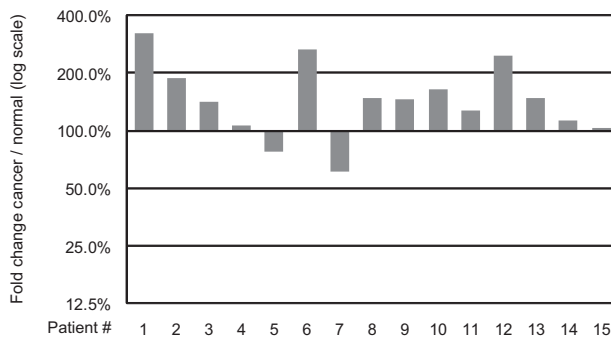
MacroH2A1 is differentially regulated in distinct human tissues and certain cancer types. Loss of macroH2A1 has been shown to predict an unfavorable prognosis in lung cancer as well as in melanoma.[10,13] To assess the
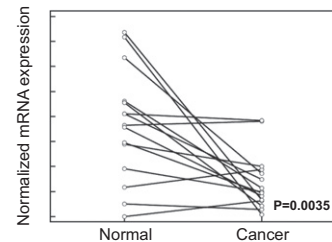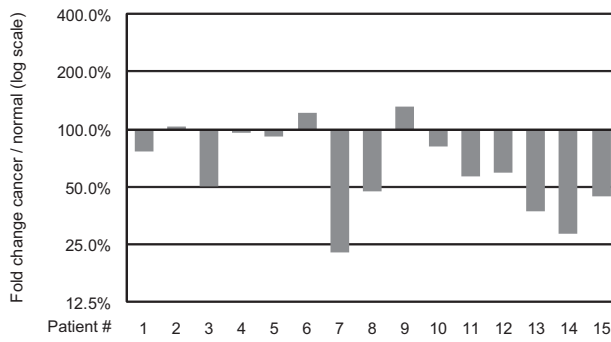
Figure 2. Opposing regulation of macroH2A1 splice variants in colon cancer and matched normal colon samples. **A:** MacroH2A1.1 mRNA is down-regulated in cancer samples compared to matched normal colon tissue (paired samples t-test, $P = 0.0035$). **B:** MacroH2A1.2 mRNA is up-regulated in cancer samples compared to matched normal colon samples (paired samples t-test, $P = 0.0112$).

A

Colon cancer sample

Tumor cells marked with pen tool
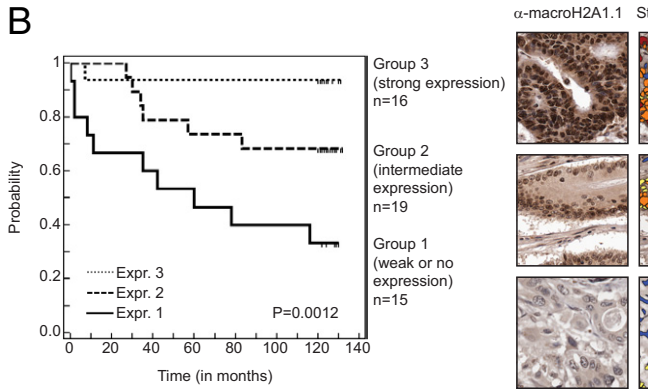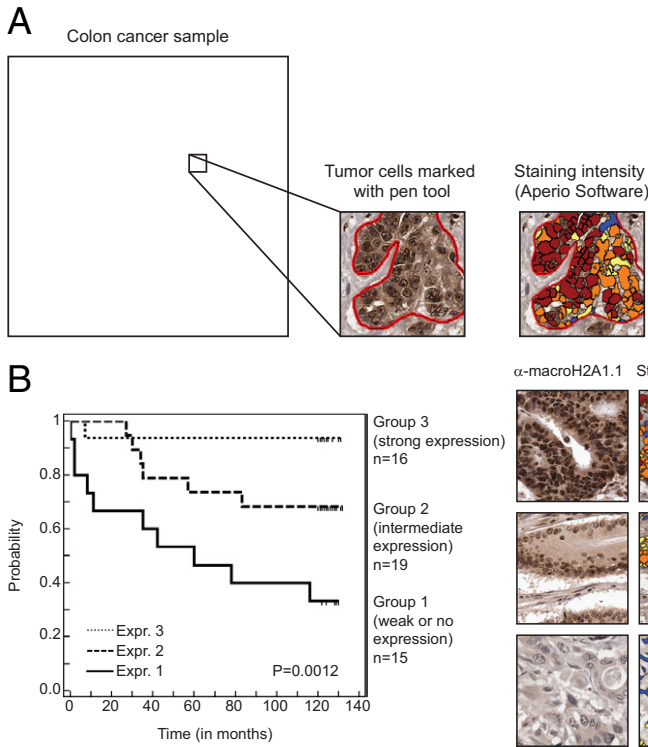
Staining intensity (Aperio Software)

Figure 3. MacroH2A1.1 protein levels predict survival in colon cancer. **A:** Paraffin-embedded tissue multiarrays containing colorectal cancer samples were assessed for macroH2A1.1 protein expression. Slides were scanned using an Aperio Scanscope XT instrument at ×20. Tumor cells within each core (**left**) were selected for analysis using the pen tool within the WebScope viewing software (**middle**). The Aperio Nuclear tool was used to measure the nuclear staining intensity of the cancer cells within each core (**right**). **B:** MacroH2A1.1 expression predicts survival in colon cancer. Three intensity levels were discerned: 1 (weak or no staining); 2 (intermediate nuclear staining); and 3 (strong nuclear staining). Representative patient samples (Patients A, B, and C) for each group (1, 2, and 3, respectively) are shown with immunohistochemistry and nuclear staining intensity side by side. Expression levels of macroH2A1.1 show a significant correlation with survival in colon cancer samples (*P* = 0.0012). **C:** Normal colon tissue shows a strong nuclear macroH2A1.1 staining.

B

C
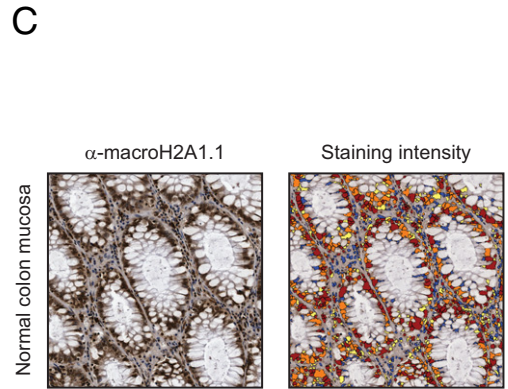
expression levels of macroH2A1 isoforms in colon cancer (Figure 1), we used specific qPCR assays to quantify the expression of macroH2A1.1 and macroH2A1.2 in human colon cancer and matched normal colon tissue samples. We found that although macroH2A1.1 levels were down-regulated when comparing cancer with normal colon samples (*P* = 0.0035) (Figure 2A), macroH2A1.2 levels were up-regulated (*P* = 0.0112) (Figure 2B). This is consistent with the idea of macroH2A1.1 as a marker of cellular differentiation and suggests distinct functions for both splice variants.

MacroH2A1.1 Expression Predicts Survival in Colon Cancer

To assess the protein expression of macroH2A1.1 and macroH2A1.2 in colon cancer samples, we performed immunohistochemistry on colon cancer samples of 50 patients from a tissue microarray. Slides were scanned, and the nuclear expression was determined by the Aperio software (Figure 3A). To determine a dependence of overall survival on expression of macroH2A1.1 in colon cancer, we performed a log-rank test in a univariate analysis. Interestingly, it revealed a significant correlation between macroH2A1.1 expression and survival (*P* = 0.0012). Patients with low macroH2A1.1 expression had a worse outcome than patients with high macroH2A1.1 levels (Figure 3B). Contrarily, expression levels of macroH2A1.2 did not show a significant correlation with survival (*P* = 0.1413) (see Supplemental Figure S1 at *http://ajp.amjpathol.org*). This is in line with findings in lung cancer that demonstrated a significant relationship be-

tween macroHA1.1 levels and lung cancer recurrence, which was not the case for macroH2A1.2.[10] Together with findings in melanoma, demonstrating an association between the global loss of macroH2A variants and an unfavorable prognosis,[13] this suggests that gradual loss of macroH2A1.1 might be a general feature in carcinogenesis influencing the respective prognosis. This not only identifies macroH2A1.1 as a novel tool of risk stratification in colon cancer patients, but also opens the prospect of a much wider use in cancer diagnostics with a potentially broad prognostic value. In accordance with our qPCR results, normal colon mucosa demonstrated a strong nuclear macroH2A1.1 staining (Figure 3C).

MacroH2A1.1 Is Up-Regulated over the Course of Differentiation

MacroH2A1.1 levels have been shown to correlate with the proliferative index of cancer samples, and it has been suggested that macroH2A1.1 levels reflect the degree of cellular differentiation.[10] Additionally, macroH2A1.1 has been shown to be up-regulated during cellular senescence, suggesting macroH2A1.1 as a marker for cells that have exited the cell cycle.[5,10] To further investigate the role of macroH2A1 isoforms during differentiation, we performed a cell culture experiment that allowed us to observe macroH2A1 levels over the course of differentiation. It has been shown that Caco-2 cells become differentiated and polarized when cultured beyond confluency under regular conditions and that their phenotype resembles enterocytes of the small intestine.[14] We harvested cells over the
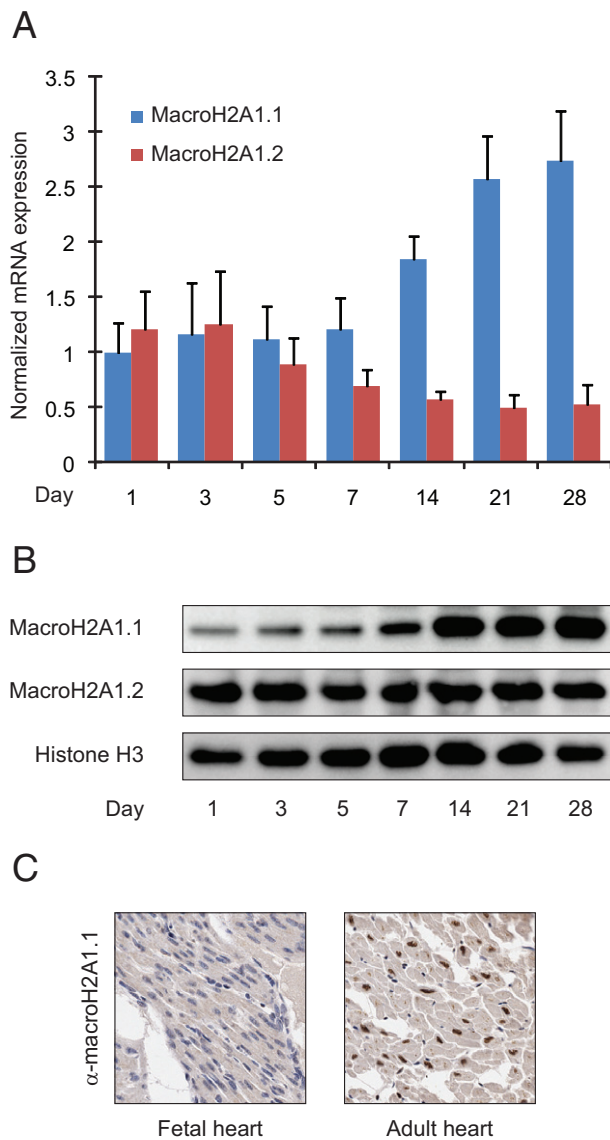
A

B

C

Figure 4. Opposing regulation of macroH2A1 splice variants over the course of differentiation of Caco-2 cells. **A:** Although macroH2A1.1 mRNA levels increase over the course of differentiation, macroH2A1.2 levels show a slight decrease. **B:** MacroH2A1.1 protein levels increase with differentiation, whereas macroH2A1.2 levels remain constant. Histone H3 serves as the loading control. **C:** Immunohistochemical staining against macroH2A1.1 reveals weak nuclear staining in fetal, but strong staining in adult heart tissue (original magnification, ×20).

course of 28 days, thus allowing us to compare cells in the log phase of active proliferation, at confluency, and after differentiation. Interestingly, we found an up-regulation of macroH2A1.1 transcript and protein over the course of the experiment, reflecting the degree of cellular differentiation (Figure 4, A and B). Notably, splice isoform macroH2A1.2 behaved differently. Although transcript levels of macroH2A1.2 slightly decreased over the course of differentiation, protein levels of macroH2A1.2 remained constant (Figure 4, A and B), which further strengthened the idea of functionally distinct roles for both splice variants. The dependence of macroH2A1.1 expression on the degree of differentiation was further supported by immunohistochemical staining of fetal and

adult heart tissue. Although adult heart revealed strong nuclear macroH2A1.1 staining, fetal heart tissue showed only weak nuclear staining (Figure 4C). These results paralleled findings in mice that showed strong staining of both variants in adult kidney and liver, but decreased macroH2A1.1 expression in the fetal counterpart.[8]

Changes in MacroH2A1.1 over the Course of Differentiation Are Reflected by Changes in Cell Cycle Regulation and Features of Cellular Senescence

To further characterize the changes accompanying the increase in macroH2A1.1 levels over the course of differentiation, we performed pathway-focused qPCR analyses using PCR arrays. PCR arrays are highly reliable tools for the expression analysis of a focused panel of genes, combining the profiling capability of microarrays with the accuracy and reliability of validated quantitative real-time PCR. We queried the transcript of 148 genes involved in cell cycle regulation and cellular senescence, and compared the expression levels of these genes in actively proliferating (day 1) and differentiated (day 21) Caco-2 cells, characterized by low and high macroH2A1.1 levels, respectively.

In differentiated cells, we found a global down-regulation of cell cycle markers crucial for cell cycle progression and proliferation involved in all phases of the cell cycle (Figure 5A). We found a down-regulation of genes associated with checkpoint and DNA damage control, as well as a down-regulation of proliferation markers resembling the state of cellular differentiation and the lack of proliferation. A few genes were up-regulated; among these were genes associated with cell cycle arrest (*CDKN1A*, *CDKN2B*, *RBL2*) and anti-proliferative or growth inhibitory action (*CCNG1*, *CCNG2*).

MacroH2A1 isoforms have been shown to be up-regulated during senescence, and macroH2A1.1 has been described as an oncogene-induced senescence marker in lung cancer development.[10] Here, we show that increase in macoH2A1.1 in Caco-2 cells coincided with exhibition of senescent features (Figure 5B). The decreased proliferative activity characteristic for senescent cells was indicated by down-regulation of genes expressing transcription factors (*E2F1*, *ETS2*, *TBX3*), cyclins (*CCNE1*, *CCNB1*, *CCNA2*), and kinases important for proliferation and growth (*CDK6*), as well as genes controlling the cell cycle (*CHEK1* and *CHEK2*, *CDK2ND*). Genes expressing tumor suppressors and associated proteins were up-regulated (*RB1*, *RBL2*, *PTEN*), whereas oncogenes were down-regulated (*MYC*, *HRAS*). We further found an up-regulation of genes involved in cell cycle arrest and growth suppression (*CDKN1A*, *CDKN1C*, *CDKN2B*, *CDKN2C*, *SPARC*), inducer of differentiation (*IRF5*, *PRKCD*), and enhancer of senescence (*CREG1*). Genes responsible for development of connective tissue (*COL1A1*, *GLB1*) were also up-regulated. On the other hand, we observed a striking down-regulation of the gene for telomerase
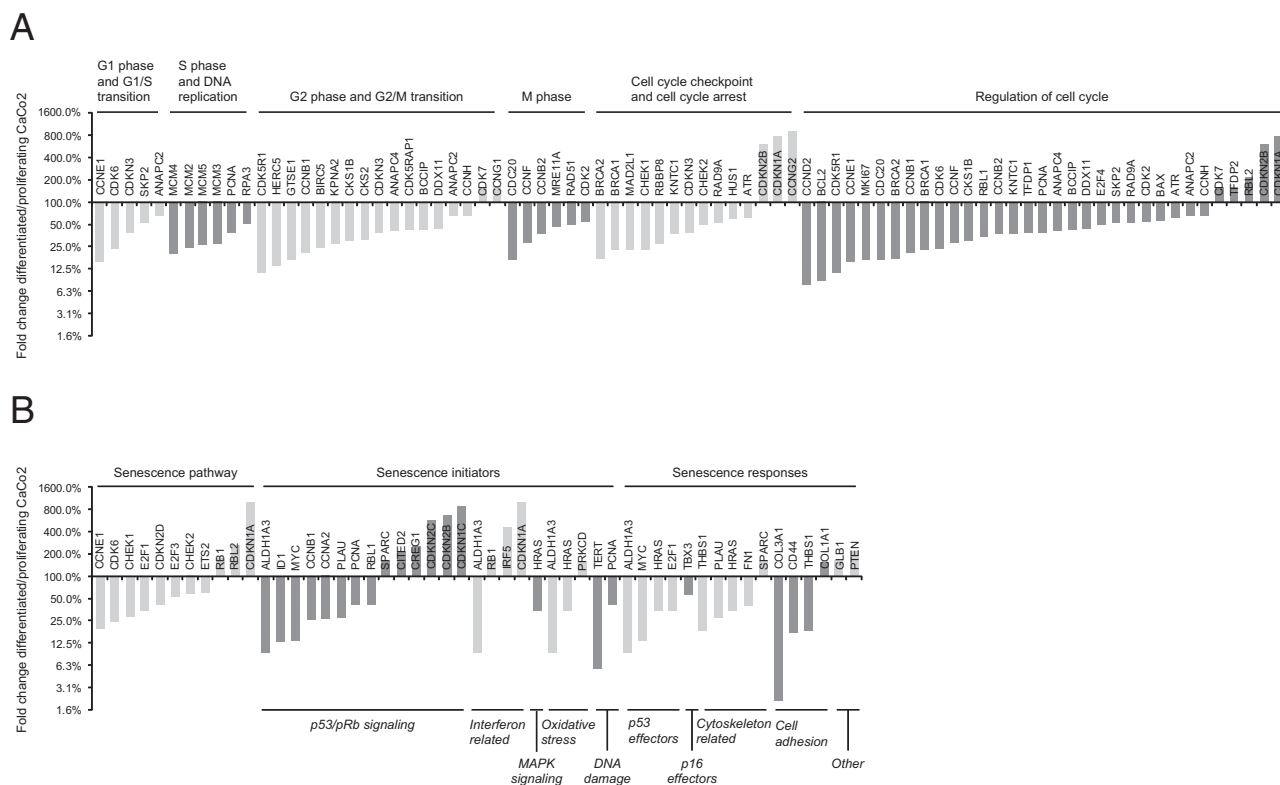
A

B

Figure 5. Changes of macroH2A1.1 are reflected by changes in cell cycle regulation and features of cellular senescence. **A:** The fold change of normalized expression between proliferating and differentiated Caco-2 cells was analyzed by pathway-focused validated qPCR arrays and reveals a down-regulation of genes associated with cell cycle progression and proliferation, in conjunction with up-regulation of growth inhibitory genes. **B:** Differentiated Caco-2 cells (high macroH2A1.1 levels) exhibit features consistent with cellular senescence. All genes with an expression change greater than ±1.5-fold along with *P* values smaller than 0.05 were depicted on the graph with a logarithmic scale. Genes belonging to more than one subgroup are named repeatedly.

(*TERT*), which is an important characteristic of cellular senescence. Inhibitor of differentiation (*ID1*) and pro-proliferative genes were down-regulated (*PCNA*, *RBL1*). Levels of collagen α-1(III) (*COL3A1*), a collagen type characteristic for fetal collagen and extracellular matrix, were strongly decreased. Interestingly, we also noted a down-regulation of genes found to be associated with migration and metastasis in other cancer types (*ALDH1A3*, *PLAU*, *FN1*, *CD44*), as well as genes with proangiogenic activity (*THBS1*), which resembles the loss of tumorigenic potential observed in differentiated Caco-2 cells.

Knockdown of MacroH2A1.1 Is Associated with a Phenotype Favoring Tumor Growth and Metastasis

To analyze the effects of loss of macroH2A1 isoforms, we performed transient knockdowns of macroH2A1.1 and macroH2A1.2 in FET cells. The FET colon carcinoma cell line is derived from an early stage human colon cancer and as such possesses properties of early malignant cells rather than advanced carcinoma cells.[15,16] FET cells are highly differentiated, but poorly invasive[17] cancer cells and show a fairly high baseline expression of macroH2A1 isoforms. Different from Caco-2 cells, FET cells do not show varying

macroH2A1 levels under regular culture conditions, making them a suitable tool for assessing the effects of macroH2A1 depletion in a cell line with a naturally high and stable expression of macroH2A1. This approach allowed us to assess the effects of varying macroH2A1 levels in a second independent cell-line model complementing the Caco-2 differentiation experiment. RNA from knockdown and control experiments was analyzed using the same PCR arrays as in the above Caco-2 differentiation experiment (Figure 5). Expression changes were calculated comparing knockdown to control cells. Overall, we observed more subtle expression changes than in the previous experiment. This was expected, as we compared two sets of cancer cells that were both proliferating, whereas previously, we compared cells with two distinct phenotypes, colon cancer cells on one hand and cells resembling enterocytes without tumorigenic potential on the other. Knockdown of macroH2A1.1 was very specific and did not lead to major changes in macroH2A1.2 levels, yet knockdown of macroH2A1.2 involved a decrease in macroH2A1.1 levels (Figure 6A).

FET cells with reduced macroH2A1.1 levels showed a phenotype consistent with enhanced proliferation and DNA replication (up-regulation of *HERC5*, *BRCA2*, *CCND2*, *HUS1*, *NBN*, and *CITED2*), favoring survival (up-regulation of apoptotic inhibitor gene *SERPINB2*, down-regulation of
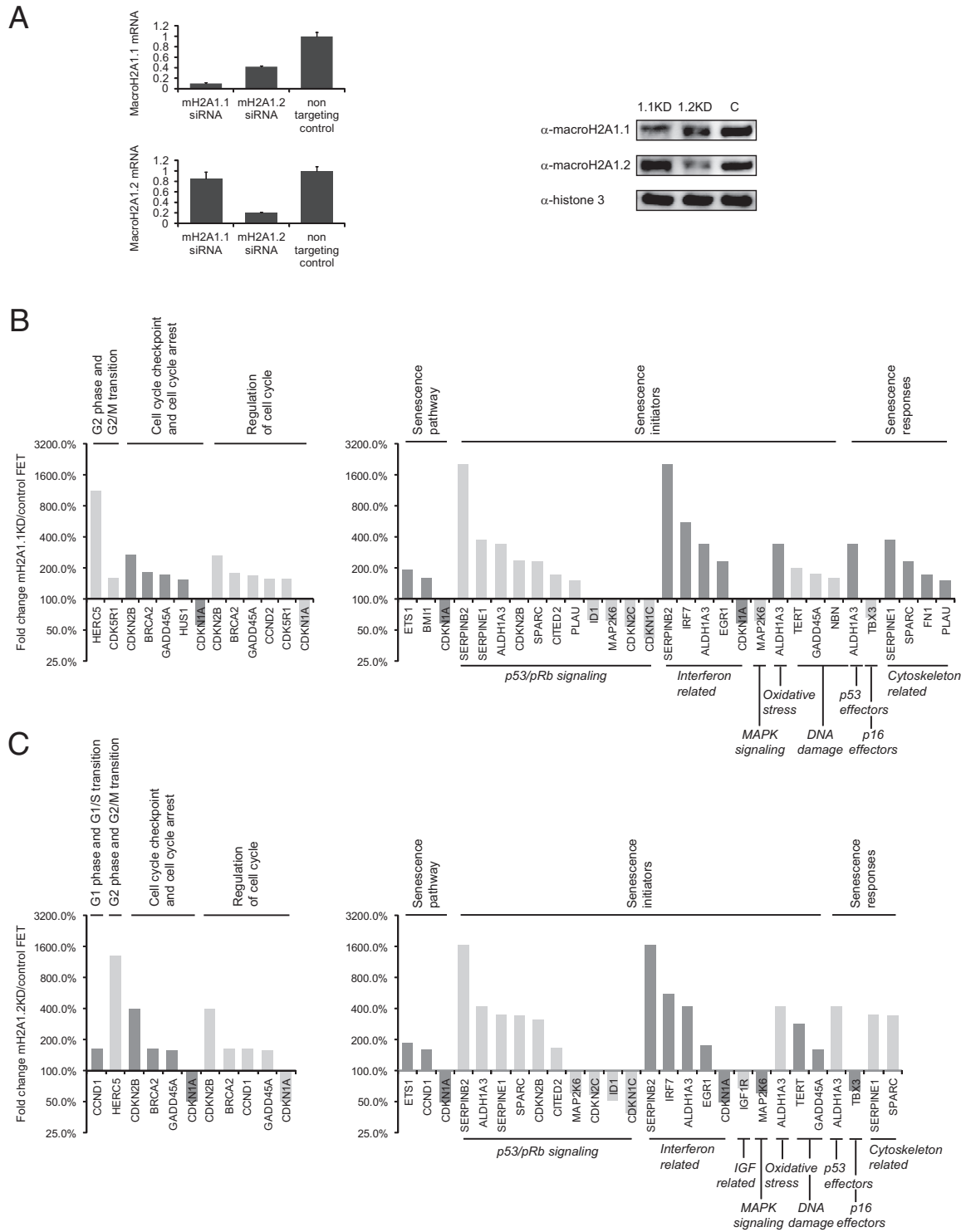
Figure 6. Knockdown of macroH2A1 isoforms is associated with a phenotype enhancing proliferation and metastasis. **A:** Transient knockdown of macroH2A1.1 and macroH2A1.2 is determined by qPCR (**left**) and Western blot analysis (**right**). **B:** Effects of macroH2A1.1 knockdown were analyzed by pathway-focused validated qPCR arrays. Expression changes are calculated comparing knockdown to control cells. **C:** Effects of macroH2A1.2 knockdown were analyzed by qPCR arrays. All genes with an expression change greater than ±1.5-fold along with *P* values smaller than 0.05 were depicted on the graph with a logarithmic scale. Genes belonging to more than one subgroup are named repeatedly.

CDKN1A), as well as a relief of gene silencing (up-regulation of *GADD45A*) (Figure 6B). Transcriptional repressors (*ID1*, *TXB3*) and markers of cell cycle arrest and growth inhibition (*CDKN1A*, *CDKN1C*, *CDKN2C*, and *MAP2K6*)

were suppressed. Surprisingly, *CDKN2B*, classically described as a cell cycle inhibitor, was up-regulated following macroH2A1.1 knockdown, whereas we had expected a down-regulation. Interestingly, these data paralleled re-

cent findings in chronic lymphocytic leukemia and small lymphocytic lymphoma showing specific overexpression of p15 (*CDKN2B*) along with up-regulation of *CCND2* in the proliferation centers of these tumors.[18] Notably, we observe an up-regulation of the gene for telomerase (*TERT*), mirroring the results of the differentiation experiment, as well as other genes with known oncogenic potential (*BMI1*, *EGR1*, *ETS1*, *HERC5*). Especially interesting is the up-regulation of several genes that have been shown to be involved in migration and metastasis in various other cancer types (*ALDH1A3*, *CDK5R1*, *FN1*, *PLAU*, *SERPINE1*, *SPARC*) (see Supplemental Table S3[18–43] at *http://ajp.amjpathol.org*).

Results of the macroH2A1.2 knockdown revealed a similar phenotype (Figure 6C). Yet, seven genes that were changed after knockdown of macroH2A1.1 were not changed after macroH2A1.2 knockdown (*CDK5R1*, *HUS1*, *CCND2*, *BMI1*, *PLAU*, *NBN*, *FN1*). Two additional genes were found to be changed (*CCND1*, *IGF1R*). Although the effects of the macroH2A1.1 knockdown can be considered specific, it is unclear whether and to what degree the results of the macroH2A1.2 knockdown are influenced by the decrease of macroH2A1.1 (Figure 6A). Thus, the similar phenotype observed could be explained either by a functional overlap of both splice variants in FET cells or by the concomitant decrease in macroH2A1.1 observed following macroH2A1.2 knockdown. In summary, we can only conclude that loss of macroH2A1.1 leads to a phenotype associated with enhanced migration, proliferation, and cell survival.

Discussion

Histones are often assumed to be expressed at similar levels in different cell types. Yet, this is not the case for macroH2A1. MacroH2A1 is unusual in several molecular and cellular features. At the structural level, it carries a huge globular domain, the *macro* domain. Further, there are two splice variants, macroH2A1.1 and macroH2A1.2, that differ in only one exon. Despite a certain overlap that has been described for the distribution and function of these isoforms, several studies point to explicit differences between macroH2A1.1 and macroH2A1.2, supporting the idea of functionally distinct isoforms.

Here, we show that whereas macroH2A1.1 is decreased in colon cancer versus matched normal colon samples at the RNA level, macroH2A1.2 expression is increased, which supports the concept of functional differences. Consistently, we find strong macroH2A1.1 protein expression in normal colon mucosa and varying expression in different colon cancer samples. Notably, only expression of macroH2A1.1 predicts outcome in colon cancer. Patients with low levels of macroH2A1.1 have a worse outcome than patients with high levels. This identifies macroH2A1.1 as a novel tool of risk stratification in colon cancer patients and establishes macroH2A1.1 as a predictive biomarker in another cancer type. Together with previous findings that characterized macroH2A1.1 as a predictor of lung cancer recurrence and showed an

association of global loss of macroH2A variants and melanoma progression,[10,13] this suggests that loss of macroH2A1.1 might be a general feature of carcinogenesis that is linked to the aggressiveness of the tumor and, thus, to the prognosis of the patient. Utilization of macroH2A1.1 as a prognostic marker might have a broad clinical application that should be addressed in future studies in more cancer types.

We further show that macroH2A1.1 increases with differentiation *in vitro*. These changes are reflected by changes of cell cycle regulation and features of cellular senescence that we characterized by pathway-focused qPCR arrays assessing 148 genes. Quantitative PCR arrays are powerful tools to determine expression changes, combining the advantage of multiple gene profiling of arrays with the sensitivity and specificity of quantification by validated real-time PCR, thus providing very reliable and reproducible data. Using this approach, we found a phenotype that is enriched for macroH2A1.1 and marked by down-regulation of genes associated with cell cycle progression and proliferation, in conjunction with up-regulation of growth inhibitory genes and genes characteristic for senescent cells. This correlates with previous results that demonstrated an enrichment of macroH2A1.1 in lung adenomas, a model of oncogene-induced senescence, along with loss of macroH2A1.1 in lung adenocarcinoma cells that had overcome senescence.[10] We conclude that macroH2A1.1 might be a general marker of cellular senescence, reflecting the degree of cellular differentiation.

Additionally, we find that loss of macroH2A1.1 is characterized by a pro-proliferative phenotype favoring cell survival, as well as migration and metastasis. Remarkably, macroH2A1.1 knockdown is associated with up-regulation of a variety of genes that have been demonstrated to play important roles in carcinogenesis and to possess prognostic potential with respect to stage, grade, metastasis, and survival in various cancer types. These data explain and strongly support the prognostic correlation between macroH2A1.1 levels and outcome that we demonstrated *in vivo*.

Colon cancer derives from an imbalance in proliferation, differentiation, and apoptosis of epithelial cells. Once proliferation predominates, benign tumors, called adenomas, emerge that are known to be enriched in senescent cells.[44] Eventually, these adenomas may evolve into cancer, and in an advanced stage, cancer cells may invade surrounding tissues and metastasize. Here, we show that macroHA1.1 is involved in the regulation of proliferation, differentiation, senescence, and migration in colon cancer, suggesting an important role in colorectal carcinogenesis and possibly in carcinogenesis in general. We demonstrate that macroH2A1.1 predicts survival in colon cancer patients, providing a novel prognostic tool for stratification of colon cancer patients. This is another step toward clinical utilization of markers that help to define individual risk signatures in patients, leading to better targeting of therapeutic strategies and ultimately improving the overall survival in cancer patients.

Acknowledgments

References

1. Pehrson JR, Fried VA: MacroH2A, a core histone containing a large nonhistone region. Science 1992, 257:1398–1400

2. Chakravarthy S, Gundimella SK, Caron C, Perche PY, Pehrson JR, Khochbin S, Luger K: Structural characterization of the histone variant macroH2A. Mol Cell Biol 2005, 25:7616–7624

3. Kustatscher G, Hothorn M, Pugieux C, Scheffzek K, Ladurner AG: Splicing regulates NAD metabolite binding to histone macroH2A. Nat Struct Mol Biol 2005, 12:624–625

4. Pehrson JR, Fuji RN: Evolutionary conservation of histone macroH2A subtypes and domains. Nucleic Acids Res 1998, 26:2837–2842

5. Zhang R, Poustovoitov MV, Ye X, Santos HA, Chen W, Daganzo SM, Erzberger JP, Serebriiskii IG, Canutescu AA, Dunbrack RL, Pehrson JR, Berger JM, Kaufman PD, Adams PD: Formation of macroH2A-containing senescence-associated heterochromatin foci and senescence driven by ASF1a and HIRA. Dev Cell 2005, 8:19–30

6. Rasmussen TP, Mastrangelo MA, Eden A, Pehrson JR, Jaenisch R: Dynamic relocalization of histone MacroH2A1 from centrosomes to inactive X chromosomes during X inactivation. J Cell Biol 2000, 150:1189–1198

7. Costanzi C, Pehrson JR: Histone macroH2A1 is concentrated in the inactive X chromosome of female mammals. Nature 1998, 393:599–601

8. Pehrson JR, Costanzi C, Dharia C: Developmental and tissue expression patterns of histone macroH2A1 subtypes. J Cell Biochem 1997, 65:107–113

9. Rasmussen TP, Huang T, Mastrangelo MA, Loring J, Panning B, Jaenisch R: Messenger RNAs encoding mouse histone macroH2A1 isoforms are expressed at similar levels in male and female cells and result from alternative splicing. Nucleic Acids Res 1999, 27:3685–3689

10. Sporn JC, Kustatscher G, Hothorn T, Collado M, Serrano M, Muley T, Schnabel P, Ladurner AG: Histone macroH2A isoforms predict the risk of lung cancer recurrence. Oncogene 2009, 28:3423–3428

11. Rozen S, Skaletsky HJ: Primer3 on the WWW for general users and for biologist programmers. Bioinformatics Methods and Protocols: Methods in Molecular Biology. Edited by Krawetz S, Misener S. Totowa NJ, Humana Press, 2000, p. pp. 365–386

12. Vandesompele J, De Preter K, Pattyn F, Poppe B, Van Roy N, De Paepe A, Speleman F: Accurate normalization of real-time quantitative RT-PCR data by geometric averaging of multiple internal control genes, Genome Biol 2002, 3:RESEARCH0034

13. Kapoor A, Goldberg MS, Cumberland LK, Ratnakumar K, Segura MF, Emanuel PO, Menendez S, Vardabasso C, Leroy G, Vidal CI, Polsky D, Osman I, Garcia BA, Hernando E, Bernstein E: The histone variant macroH2A suppresses melanoma progression through regulation of CDK8. Nature 2010, 468:1105–1109

14. Pinto MS, Robine-Leon S, Appay MD, Kedinger M, Triadou N, Dussaulx E, Lacroix B, Simon-Assmann P, Haffen K, Fogh J, Zweibaum A: Enterocyte-like differentiation and polarization of the human colon carcinoma cell line Caco-2 in culture. Biol Cell 1983, 48:323–330

15. Brattain MG, Brattain DE, Fine WD, Khaled FM, Marks ME, Kimball PM, Arcolano LA, Danbury BH: Initiation and characterization of cultures of human colonic carcinoma with different biological characteristics utilizing feeder layers of confluent fibroblasts. Oncodev Biol Med 1981, 2:355–366

16. Brattain MG, Levine AE, Chakrabarty S, Yeoman LC, Willson JK, Long B: Heterogeneity of human colon carcinoma. Cancer Metastasis Rev 1984, 3:177–191

17. Jiang W, Tillekeratne MPM, Brattain MG, Banerji SS: Decreased stability of transforming growth factor beta type II receptor mRNA in RER+ human colon carcinoma cells. Biochemistry 1997, 36:14786–14793

18. Igawa T, Sato Y, Takata K, Fushimi S, Tamura M, Nakamura N, Maeda Y, Orita Y, Tanimoto M, Yoshino T: Cyclin D2 is overexpressed in

19. Marcato P, Dean CA, Pan D, Araslanova R, Gillis M, Joshi M, Helyer L, Pan L, Leidal A, Gujar S, Giacomantonio CA, Lee PW: Aldehyde dehydrogenase activity of breast cancer stem cells is primarily due to isoform ALDH1A3 and its expression is predictive of metastasis, Stem Cells 2011, 29:32–45

20. Itahana K, Zou Y, Itahana Y, Martinez JL, Beausejour C, Jacobs JJ, Van Lohuizen M, Band V, Campisi J, Dimri GP: Control of the replicative life span of human fibroblasts by p16 and the polycomb protein Bmi-1. Mol Cell Biol 2003, 23:389–401

21. Rajan JV, Wang M, Marquis ST, Chodosh LA: Brca2 is coordinately regulated with Brca1 during proliferation and differentiation in mammary epithelial cells. Proc Natl Acad Sci U S A 1996, 93:13078–13083

22. Fu M, Wang C, Li Z, Sakamaki T, Pestell RG: Minireview: cyclin D1: normal and abnormal functions. Endocrinology 2004, 145:5439–5447

23. Lossos IS, Czerwinski DK, Alizadeh AA, Wechser MA, Tibshirani R, Botstein D, Levy R: Prediction of survival in diffuse large-B-cell lymphoma based on the expression of six genes. N Engl J Med 2004, 350:1828–1837

24. Moncini S, Salvi A, Zuccotti P, Viero G, Quattrone A, Barlati S, De Petro G, Venturin M, Riva P: The role of miR-103 and miR-107 in regulation of CDK5R1 expression and in cellular migration. PLoS One 2011, 6:e20038

25. Kranc KR, Bamforth SD, Braganca J, Norbury C, van Lohuizen M, Bhattacharya S: Transcriptional coactivator Cited2 induces Bmi1 and Mel18 and controls fibroblast proliferation via Ink4a/ARF. Mol Cell Biol 2003, 23:7658–7666

26. Virolle T, Krones-Herzig A, Baron V, De Gregorio G, Adamson ED, Mercola D: Egr1 promotes growth and survival of prostate cancer cells. Identification of novel Egr1 target genes. J Biol Chem 2003, 278:11802–11810

27. Seth A, Watson DK: ETS transcription factors and their emerging roles in human cancer. Eur J Cancer 2005, 41:2462–2478

28. Ridley A: Molecular switches in metastasis. Nature 2000, 406:466–467

29. Barreto G, Schafer A, Marhold J, Stach D, Swaminathan SK, Handa V, Doderlein G, Maltry N, Wu W, Lyko F, Niehrs C: Gadd45a promotes epigenetic gene activation by repair-mediated DNA demethylation. Nature 2007, 445:671–675

30. Grigoryev SA, Nikitina T, Pehrson JR, Singh PB, Woodcock CL: Dynamic relocation of epigenetic chromatin markers reveals an active role of constitutive heterochromatin in the transition from proliferation to quiescence. J Cell Sci 2004, 117:6153–6162

31. Volkmer E, Karnitz LM: Human homologs of Schizosaccharomyces pombe rad1, hus1, and rad9 form a DNA damage-responsive protein complex. J Biol Chem 1999, 274:567–570

32. Marie I, Durbin JE, Levy DE: Differential viral induction of distinct interferon-alpha genes by positive feedback through interferon regulatory factor-7. EMBO J 1998, 17:6660–6669

33. Wilda M, Demuth I, Concannon P, Sperling K, Hameister H: Expression pattern of the Nijmegen breakage syndrome gene. Nbs1, during murine development. Hum Mol Genet 2000, 9:1739–1744

34. Harbeck N, Kates RE, Gauger K, Willems A, Kiechle M, Magdolen V, Schmitt M: Urokinase-type plasminogen activator (uPA) and its inhibitor PAI-I: novel tumor-derived factors with a high prognostic and predictive impact in breast cancer. Thromb Haemost 2004, 91:450–456

35. Dickinson JL, Bates EJ, Ferrante A, Antalis TM: Plasminogen activator inhibitor type 2 inhibits tumor necrosis factor alpha-induced apoptosis. Evidence for an alternate biological function. J Biol Chem 1995, 270:27894–27904

36. Minn AJ, Gupta GP, Siegel PM, Bos PD, Shu W, Giri DD, Viale A, Olshen AB, Gerald WL, Massague J: Genes that mediate breast cancer metastasis to lung. Nature 2005, 436:518–524

37. Shay JW, Zou Y, Hiyama E, Wright WE: Telomerase and cancer. Hum Mol Genet 2001, 10:677–685

38. Bendjennat M, Boulaire J, Jascur T, Brickner H, Barbier V, Sarasin A, Fotedar A, Fotedar R: UV irradiation triggers ubiquitin-dependent degradation of p21(WAF1) to promote DNA repair. Cell 2003, 114:599–610

39. Lee MH, Reynisdottir I, Massague J: Cloning of p57KIP2, a cyclin-dependent kinase inhibitor with unique domain structure and tissue distribution. Genes Dev 1995, 9:639–649

40. van Veelen W, Klompmaker R, Gloerich M, van Gasteren CJ, Kalk-hoven E, Berger R, Lips CJ, Medema RH, Hoppener JW, Acton DS: P18 is a tumor suppressor gene involved in human medullary thyroid carcinoma and pheochromocytoma development. Int J Cancer 2009, 124:339–345

41. Passiatore G, Gentilella A, Rom S, Pacifici M, Bergonzini V, Peruzzi F: Induction of Id-1 by FGF-2 involves activity of EGR-1 and sensitizes neuroblastoma cells to cell death, J Cell Physiol 226:1763-1770

42. Hui L, Bakiri L, Mairhorfer A, Schweifer N, Haslinger C, Kenner L, Komnenovic V, Scheuch H, Beug H, Wagner EF: p38alpha sup-presses normal and cancer cell proliferation by antagonizing the JNK-c-Jun pathway. Nat Genet 2007, 39:741–749

43. Jerome-Majewska LA, Jenkins GP, Ernstoff E, Zindy F, Sherr CJ, Papaioannou VE: Tbx3, the ulnar-mammary syndrome gene, and Tbx2 interact in mammary gland development through a p19Arf/p53-independent pathway. Dev Dyn 2005, 234:922–933

44. Collado M, Gil J, Efeyan A, Guerra C, Schuhmacher AJ, Barradas M, Benguria A, Zaballos A, Flores JM, Barbacid M, Beach D, Serrano M: Tumour biology: senescence in premalignant tumours. Nature 2005, 436:642